

# A Silurian placoderm with osteichthyan-like marginal jaw bones

Min Zhu<sup>1</sup>, Xiaobo Yu<sup>1,2</sup>, Per Erik Ahlberg<sup>3</sup>, Brian Choo<sup>1</sup>, Jing Lu<sup>1</sup>, Tuo Qiao<sup>1</sup>, Qingming Qu<sup>3</sup>, Wenjin Zhao<sup>1</sup>, Liantao Jia<sup>1</sup>, Henning Blom<sup>3</sup> & You'an Zhu<sup>1</sup>

The gnathostome (jawed vertebrate) crown group comprises two extant clades with contrasting character complements. Notably, Chondrichthyes (cartilaginous fish) lack the large dermal bones that characterize Osteichthyes (bony fish and tetrapods). The polarities of these differences, and the morphology of the last common ancestor of crown gnathostomes, are the subject of continuing debate. Here we describe a three-dimensionally preserved 419-million-year-old placoderm fish from the Silurian of China that represents the first stem gnathostome with dermal marginal jaw bones (premaxilla, maxilla and dentary), features previously restricted to Osteichthyes. A phylogenetic analysis places the new form near the top of the gnathostome stem group but does not fully resolve its relationships to other placoderms. The analysis also assigns all acanthodians to the chondrichthyan stem group. These results suggest that the last common ancestor of Chondrichthyes and Osteichthyes had a macromeric dermal skeleton, and provide a new framework for studying crown gnathostome divergence.

The early fossil record of gnathostomes is dominated by four seemingly well-defined groups: the Chondrichthyes and Osteichthyes, which are still extant, and the extinct Placodermi and Acanthodii<sup>1–9</sup>. Osteichthyan and placoderms have macromeric dermal skeletons dominated by large bony plates<sup>4,7</sup>, but these skeletons have usually been regarded as non-homologous a priori and given different nomenclatures<sup>10</sup>, because of perceived fundamental differences between placoderm and osteichthyan dermal bone patterns<sup>1,2,7,11</sup>. Chondrichthyans and acanthodians have micromeric dermal skeletons composed principally of scales. The current consensus is that placoderms are members of the gnathostome stem group<sup>11–16</sup> and most probably form a paraphyletic stem segment<sup>15,16</sup>. Recent phylogenetic analyses<sup>15,16</sup> have also recovered acanthodians as a paraphyletic assemblage spanning the chondrichthyan and osteichthyan stem groups and the crownward end of the gnathostome stem group (Fig. 1). This phylogenetic pattern implies that the macromeric dermal skeleton of placoderms was replaced by a micromeric condition in the common ancestor of crown gnathostomes, with subsequent *de novo* acquisition of a non-homologous macromeric skeleton in osteichthyans. However, the presence of placoderm-like features in the earliest osteichthyans (for example, dermal pelvic girdles<sup>17</sup> and multipartite dermal shoulder girdles with spinal plates<sup>18–20</sup>) suggests a conservation of pattern between the placoderm and osteichthyan macromeric dermal skeletons<sup>4,21–23</sup>. Homology of these skeletons would imply that the crown gnathostome node condition includes a macromeric dermal skeleton, and that the micromeric condition of acanthodians and chondrichthyans is derived (Fig. 1). The resolution of this issue hinges on the phylogenetic placement of an array of problematic fossil taxa, many yielding limited anatomical data.

Here we present a new fish from the Silurian of China<sup>20,24,25</sup> that combines a placoderm-like dermal skull roof, braincase and shoulder girdle with osteichthyan-like dermal bones of the mandibular and hyoid arches<sup>2</sup> and a palatoquadrate sharing derived characteristics with crown gnathostomes<sup>12</sup>. As this character combination has never been observed before, our description below uses placoderm terms for

the skull roof and trunk armour<sup>26</sup>, but osteichthyan terms for the dermal bones of the mandibular and hyoid arches (Supplementary Table 1).

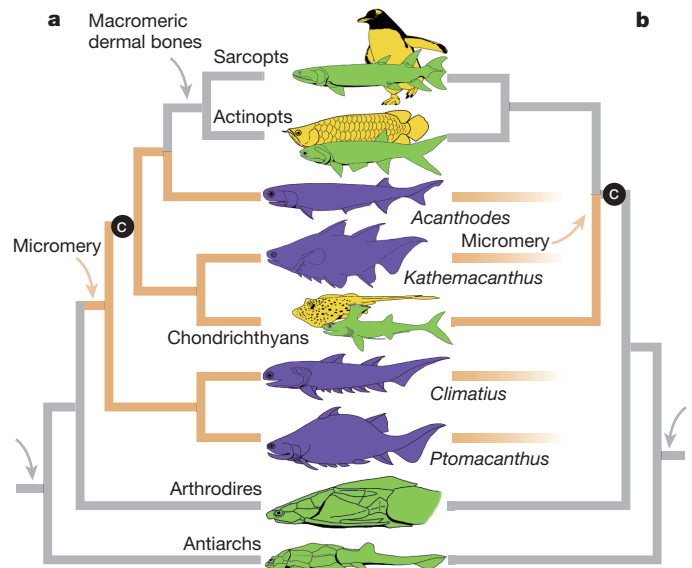


**Figure 1 | Competing hypotheses of dermal skeleton condition at the crown gnathostome node.** **a**, Simplified gnathostome phylogeny based on ref. 16. The micromeric condition (brown branches) in acanthodians (purple) and chondrichthyans brackets the crown gnathostome node (C). The macromeric condition (grey branches) is proposed as non-homologous in osteichthyans (sarcophs and actinopterygians) and placoderms (for example, arthrodiros and antiarchs). **b**, Inferred macromeric condition at the crown gnathostome node (C), as suggested by recent findings supporting placoderm-osteichthyan dermal skeleton homology. This implies that micromery in acanthodians and chondrichthyans is derived, and questions the positions of acanthodians as stem gnathostomes and stem osteichthyans.

<sup>1</sup>Key Laboratory of Vertebrate Evolution and Human Origins of Chinese Academy of Sciences, Institute of Vertebrate Paleontology and Paleoanthropology, Chinese Academy of Sciences, Beijing 100044, China. <sup>2</sup>Department of Biological Sciences, Kean University, Union, New Jersey 07083, USA. <sup>3</sup>Subdepartment of Evolution and Development, Department of Organismal Biology, Evolutionary Biology Centre, Uppsala University, Uppsala 752 36, Sweden.

## Systematic palaeontology

Gnathostomata Gegenbaur, 1874

*Entelognathus primordialis* gen. et sp. nov.

**Etymology.** The generic name derives from the Greek *enteles* (complete) and *gnathos* (jaw), referring to the complete set of dermal marginal jaw bones. The specific name is from the Latin *primordialis* (primordial).

**Holotype.** IVPP V18620, an articulated fish with head shield and trunk armour (Fig. 2a–d and Supplementary Figs 13–17 and 21a, b).

**Referred material.** Skulls, V18621.1–15; sclerotic rings, V18622.1–2; cheek–palatoquadrate complexes, V18622.3–10; trunk armour plates, V18622.11–30.

**Locality and horizon.** Xiaoxiang Reservoir, Qujing, Yunnan, China; Kuanti Formation. Late Ludlow, Silurian, *Ozarkodina snajdri* Conodont Zone, 419 million years ago<sup>20,24,25</sup>.

**Diagnosis.** A jawed stem gnathostome combining placoderm-like skull roof and trunk armour with osteichthyan-like marginal jaw bones (premaxilla, maxilla and dentary) and operculogular series. Skull roof lacking preorbital plates, premedian plate ventrally positioned between rostral and premaxilla, main lateral line meeting postmarginal line in anterior paranuchal plate, small orbital fenestra enclosed by a large oblong tripartite sclerotic ring, and anterior lateral plate with deep posterior notch for pectoral fenestra.

**Description.** The holotype represents a three-dimensionally preserved fish with articulated head shield and trunk armour, approximately 11 cm long, suggesting a total body length of over 20 cm.

### Skull roof and sclerotic ring

The skull roof is flat mesially and strongly arched laterally. Pineal, central and nuchal plates cover most of the braincase along the midline, flanked by paired postorbital, marginal, and anterior and posterior paranuchal plates along the trajectory of the infraorbital and main lateral line grooves. The large hexagonal central plate seems to have a single ossification centre, whereas most placoderms have paired centrals<sup>1,2,7</sup>. Its location anterior to the nuchal aligns *Entelognathus* with arthrodires, in which paired centrals meeting in the midline occupy the corresponding position. In acanthothoracids and petalichthyids, the nuchal extends forwards medially to separate the centrals<sup>3,4,26</sup>. The posterior margin of the nuchal is overlapped by a partially exposed short bone, here termed ‘postnuchal’ (Supplementary Figs 11 and 18a–c),

which resembles the ‘extrascapular’ of the arthrodire *Sigaspis*<sup>27</sup> and the petalichthyid *Eurycaraspis*<sup>28</sup>. The main lateral line joins the postmarginal line in the anterior paranuchal, not in the marginal as in other placoderms. The groove for the supraorbital line, with its associated postnasal and preorbital plates, is absent. No foramen for the endolymphatic duct or the pineal organ is visible.

The short and narrow snout comprises a rostral, a premedian and premaxillae (Figs 2, 3, 4i–k and 5, Supplementary Fig. 20 and Supplementary Video) that appear to be fused mesially. The rostral bends ventrally, giving the snout a near-vertical profile. A single pair of subtriangular nasal openings lies between the rostral and the sclerotic ring. The premaxilla has a narrow facial lamina, and a broad palatal lamina that flares out posteriorly and articulates with the palatal lamina of the maxilla. The facial lamina anteriorly forms a conjoined flush surface with the premedian and posteriorly contacts the lacrimal and the maxilla. The tubercles on the palatal lamina are smaller than those on the facial lamina, and somewhat tooth-like in shape. No separate vomer (or anterior supragnathal of placoderms) is present.

The small orbital fenestra is enclosed by a large oblong sclerotic ring, which comprises three intimately fused sclerotic plates (Figs 2, 3 and 4e, i–k) as in antiarchs<sup>29</sup>. The ring has sutural contacts to the adjacent skull roof bones, with an anterior process embraced by the premedian and premaxilla.

### Dermal cheek, operculogular and jaw bones

The cheek complex comprises the jugal (placoderm suborbital), lacrimal, maxilla and a possible quadratojugal (Fig. 3), and has a sensory canal pattern broadly resembling that of arthrodires<sup>23,30</sup>.

The elongate jugal has loose anterior contacts with the sclerotic ring and lacrimal, but its ventral suture with the maxilla is so tight that the bones are difficult to distinguish except by their ornament patterns. The infraorbital canal enters the jugal dorsally, runs ventrally to join the supraorbital canal, and then continues anteroventrally via the slender lacrimal to terminate below the orbit. The supraorbital canal runs posteroventrally to enter the facial lamina of the maxilla.

The maxilla has a slender facial lamina and a broad palatal lamina (Fig. 4a–d and Supplementary Figs 21, 22). At a level corresponding to the anterior margin of the fossa for adductor mandibular muscle, the ventral margin of the maxilla presents a sharp vertical bend. Anterior

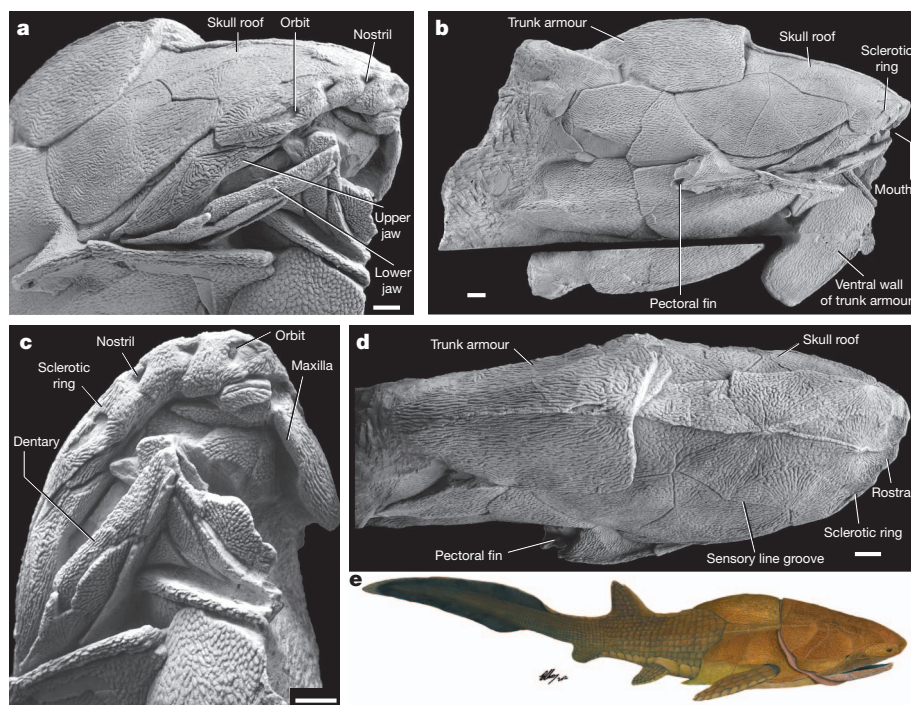


**Figure 2** | *Entelognathus primordialis* gen. et sp. nov., a 419-million-year-old jawed fish from the Kuanti Formation (Late Ludlow, Silurian), Qujing, Yunnan. a–d, Holographs of the holotype (V18620), a three-dimensionally preserved specimen with head and trunk armour in anterolateral (a), lateral (b), anteroventral (c) and dorsal (d) views. A small part of the left trunk armour was accidentally sawed off as extraneous material and repositioned in b. Scale bars, 1 cm. e, Life restoration.

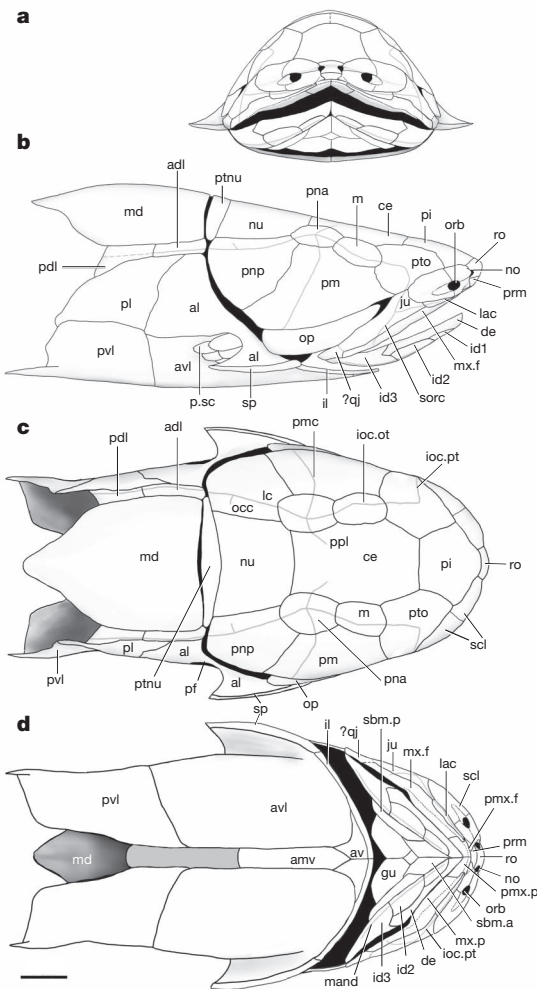


**Figure 3** | *Entelognathus primordialis* gen. et sp. nov. **a–d**, Restoration of the dermal skeleton in anterior (**a**), lateral (**b**), dorsal (**c**) and ventral (**d**) views. Scale bars, 1 cm. adl, anterior dorsolateral plate; al, anterior lateral plate; amv, anterior medioventral plate; av, anteroventral plate; avl, anterior ventrolateral plate; ce, central plate; de, dentary; gu, principal gular; id1–3, first to third infradentary; il, interlateral plate; ioc.ot, otic branch of infraorbital line groove; ioc.pt, postorbital branch of infraorbital line groove; ju, jugal; lac, lacrimal; lc, main lateral line groove; m, marginal plate; mand, mandibular line groove; md, median dorsal plate; mx.f, facial lamina of maxilla; mx.p, palatal lamina of maxilla; no, nostril; nu, nuchal plate; occ, occipital cross commissure; op, opercular; orb, orbital fenestra; pdl, posterior dorsolateral plate; pf, pectoral fenestra; pi, pineal plate; pl, posterior lateral plate; pm, postmarginal plate; pmc, postmarginal line groove; pmx.f, facial lamina of premaxilla; pmx.p, palatal lamina of premaxilla; pna, anterior paranuchal plate; pnp, posterior paranuchal plate; ppl, posterior pitline; prm, premedian; ptnu, postnuchal plate; pto, postorbital plate; pvl, posterior ventrolateral plate; p.sc, pectoral fin scales; qj, quadratojugal; ro, rostral plate; sbm.a, anterior submandibular; sbm.p, posterior submandibular; scl, sclerotic plate; sorc, supraoral line groove; sp, spinal plate.

to this bend, the palatal lamina extends forward to join the palatal lamina of the premaxilla, forming a continuous horizontal shelf inward of the jaw margin, against which the mandible occludes. Elongate tubercles on the facial lamina of the maxilla and nearby dermal bones grade into close-packed rounded tubercles on the horizontal shelf. There seems to be no teeth or cusps along the oral margin. No separate dermal bones (dermopalatines, ectopterygoids or posterior supragathals of placoderms) are found medial to the maxilla.

A small, roughly triangular ossification, tentatively identified as a quadratojugal, lies at the posterior tip of the cheek complex, and is firmly sutured with the adjacent maxilla and jugal. The position of

this bone resembles that of a placoderm postsuborbital. X-ray tomography shows that the partially exposed opercular (placoderm submarginal) is an elongate crescentic bone with an opercular cartilage attached to its inner surface (Figs 2 and 3 and Supplementary Fig. 18).

The mandible (Figs 2a–c, 3a, b, d and 4i–j and Supplementary Fig. 13) is covered externally by a relatively short, edentulous dentary and three infradentaries. The dentary has a deep facial lamina but only a narrow edge dorsally, with no mesial lamina corresponding to the palatal lamina of the maxilla. No separate dermal bones (coronoids and prearticular, or infragnathals of placoderms) are found on the mesial surface of the mandible. X-ray tomography shows the mandibular line groove running through infradentary 2, and confirms the presence of the submandibular and gular series in the holotype (Fig. 4i and Supplementary Fig. 23). Medial to the infradentaries, the elongate anterior and posterior submandibulars as well as a lozenge-shaped median gular are preserved *in situ*, whereas the paired principal gulars are anteriorly displaced. Overall, this arrangement recalls the pattern seen in the lungfish *Scaumenacia*<sup>2</sup>.

### Trunk armour

The long trunk armour resembles that of early arthrodires such as a phlyctaeniid<sup>30</sup>. The anterior dorsolateral plate bears a flat anterior flange (Supplementary Fig. 26c). Coupled with the lack of an articular fossa or condyle on the posterior margin of the paranuchal plate, this flange indicates a sliding dermal neck joint as in actinolepids, phyllolepid and *Wuttagoonaspis*<sup>3,26</sup>. The anterior lateral plate (Supplementary Fig. 15a) has extensive overlap surfaces for the skull roof and the opercular, and a deep posterior notch for the pectoral fenestra. The narrow spinal and the adjoining plates form a triangular cutwater immediately anterior to the pectoral fin. The posterior ventrolateral plates have pointed tips protruding posterolaterally. Their medial margins diverge posteriorly and lack overlap surfaces, indicating that the ventral side of the trunk armour may have been incompletely enclosed posteriorly.

### Braincase

The perichondrally ossified braincase (Fig. 5) is broad and flattened, resembling that of early arthrodires<sup>23,30</sup>. Anteriorly, the ectethmoid process lies slightly posteroventral to the nasal capsule. The orbital cavity is posteriorly separated from the postorbital fossa by a pila-like structure (Fig. 5a, c, d). Behind it lies a developed postorbital fossa. The anterior postorbital process carries an oval unfinished articular facet for the hyomandibula. Medial to this facet is a small foramen for the hyomandibular trunk of the facial nerve. The otico-occipital portion makes up about two thirds of the braincase length. In contrast to ptyctodonts with three endocranial ossifications<sup>31</sup>, *Entelognathus* resembles other placoderms in lacking basicranial and otico-occipital fissures (Fig. 5a and Supplementary Fig. 19a, c, e). Behind the posterior postorbital process, the braincase tapers to form a large cuticular fossa, and carries a lateral groove for the jugular vein. There is a strong posterolaterally-oriented craniospinal process, but no supravagal process.

### Palatoquadrate

The perichondrally ossified palatoquadrates of partly disarticulated skulls (Fig. 5a and Supplementary Fig. 19e) show that the ethmoid articulation abuts the ectethmoid process of the braincase. The jaw articulation comprises a prearticular process and a quadrate concavity (Fig. 4b–d), as in acanthodians and chondrichthyans<sup>2</sup>, but unlike the bipartite convex articulation in osteichthyans<sup>32</sup>. The metapterygoid region of the palatoquadrate is expanded ventrally into a commissural lamina that confines the adductor musculature mesially (Figs 4b–d and 6b), as in crown gnathostomes<sup>12</sup>. X-ray tomography of an isolated cheek-palatoquadrate complex (Fig. 4f, g and Supplementary Fig. 22e–h) reveals the adductor chamber. Rather than being wide open anteriorly as in osteichthyans (where the metapterygoid and autopalatine attachments of the palatoquadrate on the cheek are completely

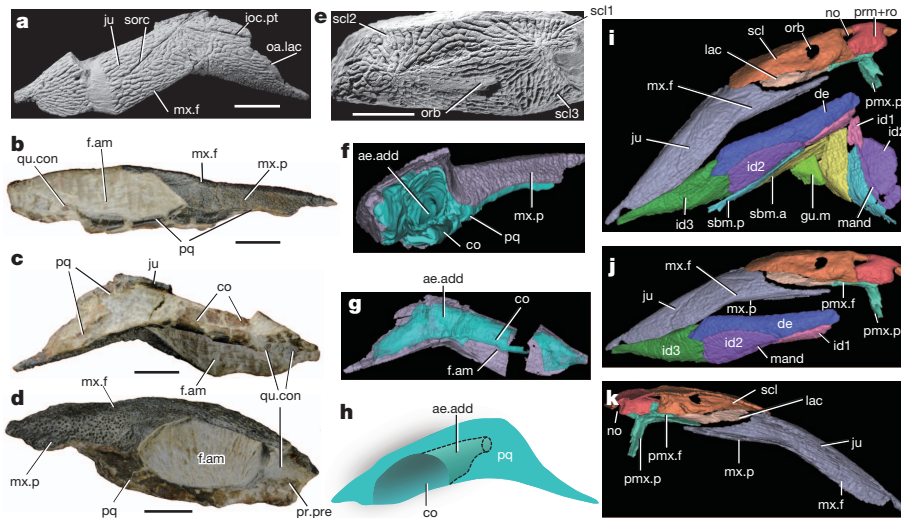


**Figure 4** | *Entelognathus primordialis* gen. et sp. nov. **a–c**, Right upper jaw in external (**a**), ventral (**b**) and medioventral (**c**) views, V18622.3. **d**, Left upper jaw in ventral view, V18622.4. **e**, Disarticulated sclerotic ring, V18622.1. **f, g**, Computerized tomography restorations of an isolated cheek-palatoquadrate complex in posterior (**f**) and medioventral (**g**) views, V18622.3; the palatoquadrate rendered semi-transparent in **g** to show the anterior tunnel-like extension of the adductor chamber. **h**, Restoration of the palatoquadrate in

lateral view. **i–k**, Computerized tomography restorations of the holotype V18620 showing the lower and upper jaws and neighbouring bones. Right side in anteroventral (**i, j**) and internal (**k**) views. Scale bars, 5 mm. ae.add, anterior extension of adductor chamber; co, commissural lamina; f.am, fossa for adductor mandibulae muscle; gu.m, median gular; oa.lac, overlapped area by lacrimal; pq, palatoquadrate; pr.pre, prearticular process; qu.con, quadrate concavity; scl1–3, first to third sclerotic plate. Other abbreviations as in Fig. 3.

separate), it has a tunnel-like anterior extension that traverses the palatoquadrate and emerges on its mesial face. A similar configuration exists in many arthrodires including *Buchanosteus*<sup>33</sup> and probably *Dicksonosteus*<sup>30</sup>.

**Phylogenetic relationship**

To explore the phylogenetic position of *Entelognathus* and the impact of its characters on gnathostome phylogeny, we conducted analyses using a modified version of the data set of ref. 16 with 253 characters

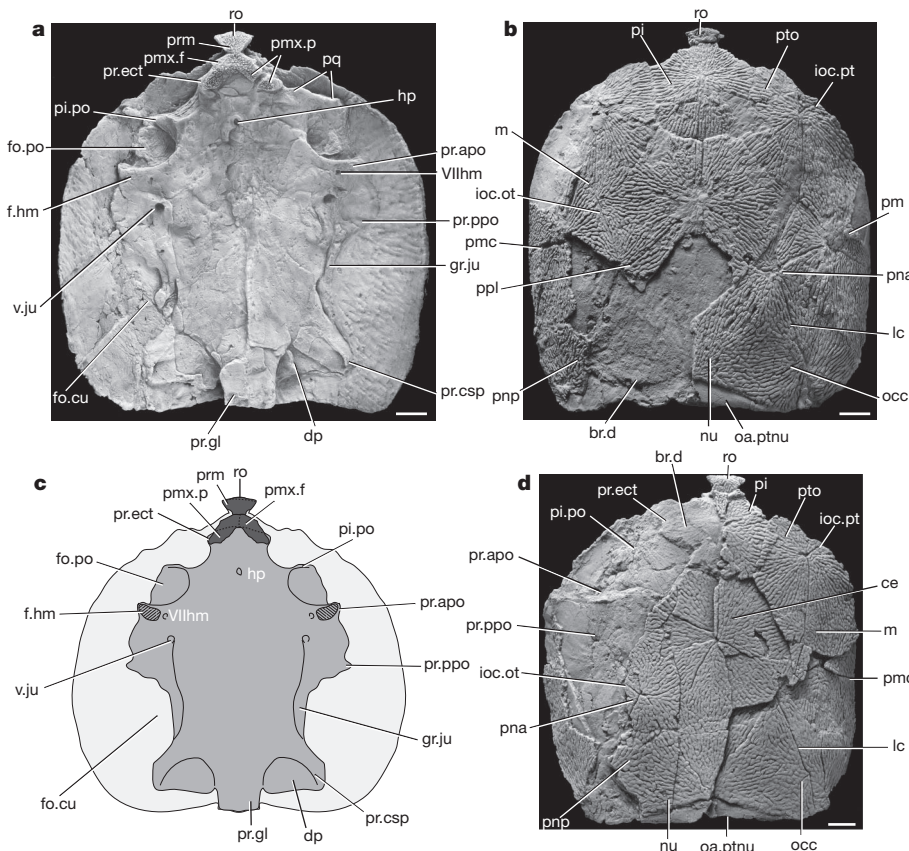


**Figure 5** | Skull roof and braincase of *Entelognathus primordialis* gen. et sp. nov. **a–b**, Skull in dorsal (**a**) and ventral (**b**) views, V18621.1. **c**, Restoration of the skull in ventral view. **d**, Skull in dorsal view, with part of skull roof removed to show the dorsal wall of braincase, V18621.2. Scale bars, 5 mm. br.d, dorsal wall of braincase; dp, depression in occipital portion of braincase; fo.cu, cuccularis fossa; fo.po, postorbital fossa; f.hm, hyomandibular facet; gr.ju, groove for jugular vein; hp, hypophysial opening; oa.ptnu, overlapped area by postnuchal plate; pi.po, postorbital pila; pr.apo, anterior postorbital process; pr.csp, craniospinal process; pr.ect, ectethmoid process; pr.gl, occipital glenoid process; pr.ppo, posterior postorbital process; v.ju, opening for jugular vein; VIIhm, hyomandibular trunk of facial nerve. Other abbreviations as in Figs 3 and 4.

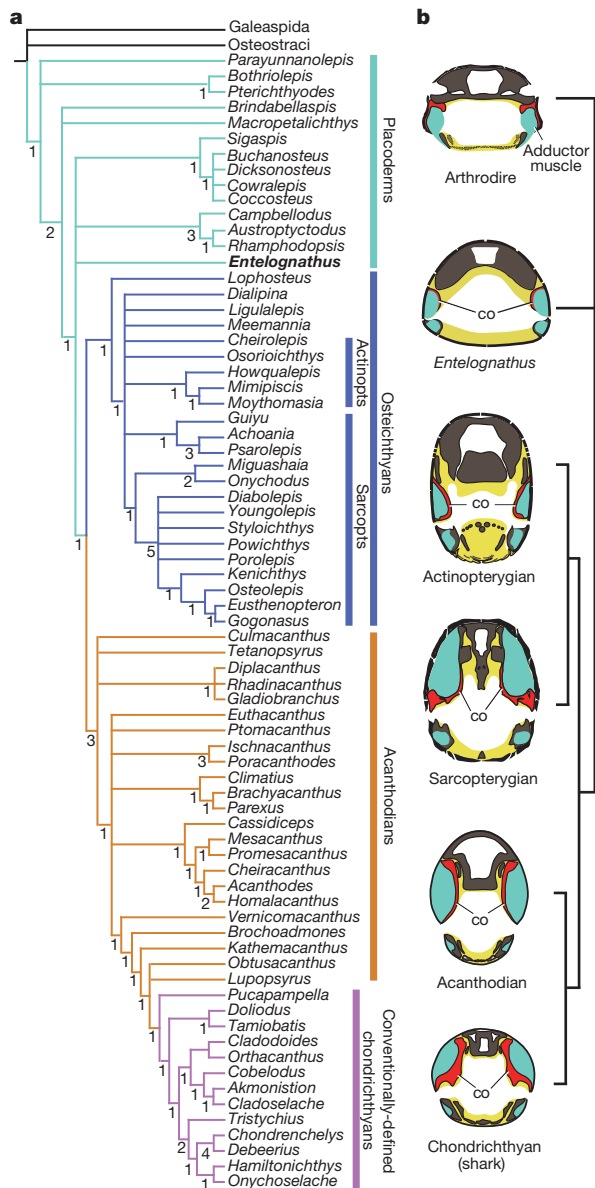


**Figure 6 | Results of phylogenetic analysis and palatoquadrate conditions among major gnathostome groups.** **a**, Strict consensus of 1,117 most parsimonious trees resulting from a modified data set. *Entelognathus* is placed in a polychotomy with arthrodires, ptyctodonts and crown gnathostomes, whereas all acanthodian taxa fall on the chondrichthyan stem. Numbers at nodes represent Bremer decay indices. **b**, Diagrammatic reconstruction of head in transverse section through the fossa for adductor mandibulae muscle to show the relationships of the braincase, palatoquadrate (red) and adductor muscle (green). *Entelognathus* resembles crown gnathostomes in having a developed commissural lamina (co). Schematic drawings modified from ref. 12.

and 75 taxa (see Supplementary Information and Methods). The strict consensus of 1,117 most parsimonious trees (MPTs) places *Entelognathus* in a polychotomy with arthrodires, ptyctodonts and crown gnathostomes (Fig. 6a), whereas the 50% majority-rule consensus favours *Entelognathus* as the sister group of crown gnathostomes (Supplementary Fig. 2a). Notably, our result differs from those of refs 15 and 16 in placing all acanthodians on the chondrichthyan stem, although it agrees with them with regard to placoderm paraphyly, osteichthyan monophyly and the internal topology of conventionally defined chondrichthyan.

### Homology of macromeric skeletons

Because the analysis of ref. 16 placed some acanthodians in the osteichthyan and gnathostome stem groups, the phenetic similarities between

acanthodians and chondrichthyan were interpreted as symplesiomorphies. Our phylogenetic result indicates that the similarities actually represent synapomorphies of the chondrichthyan total group; examples include body scales with a neck and bulging base, and a skull roof comprising undifferentiated plates or tesserae (Fig. 6a). Placement of all acanthodians in the chondrichthyan stem group also implies macromery in the last common ancestor of crown gnathostomes. Although partial to complete loss of macromery in acanthodians and chondrichthyan is implicit both in our phylogeny and those of refs 15 and 16, as a corollary of placoderm paraphyly, the important difference is whether osteichthyan macromery is a novelty or a retained primitive feature. The partly micromeric condition in the cheek and jaws of the stem osteichthyan *Dialipina*<sup>34</sup> could be interpreted as evidence for *de novo* evolution of macromery, but its skull roof pattern resembles those of both arthrodires and crown osteichthyan (Supplementary Fig. 10), suggesting homology across the gnathostome crown group node. Micromeric regions also occur between the large skull plates of some placoderms (for example, *Gemuendina*<sup>1,2</sup>), and in the snouts of many sarcopterygians (for example, *Powichthys*<sup>2</sup>). The significance of these occurrences needs to be investigated further, as does the broader question of placoderm-osteichthyan skeletal pattern homology (Supplementary Information).

### Dermal jaw and palatoquadrate evolution

Until now, dermal marginal jaw bones (premaxilla, maxilla and dentary) were regarded as key synapomorphies of Osteichthyes<sup>32,35</sup>, and have never been found in any placoderms. The similarity in shape and topographic correspondence between the marginal jaw bones of *Entelognathus* and osteichthyan strongly suggest their homology. However, unlike the question of macromery versus micromery, dermal jaw homology cannot be resolved unambiguously from our phylogenetic analysis. Three positions are recovered for *Entelognathus*, as sister group to crown gnathostomes (66% of MPTs), in a clade with arthrodires and ptyctodonts (28% of MPTs), and as sister group to ptyctodonts plus crown gnathostomes (6% of MPTs) (Supplementary Fig. 4). Only in the first topology does one of two equally parsimonious character optimizations identify the dermal jaw bones of *Entelognathus* as homologous with those of osteichthyan. This lack of resolution stems partly from gaps in the data set and partly from incongruent character distributions among key taxa, notably between *Entelognathus*, ptyctodonts and crown gnathostomes.

If the most frequently resolved position of *Entelognathus* as the sister group of crown gnathostomes (Supplementary Fig. 2a) is accepted as a working hypothesis, it offers a new perspective on the early evolution of crown gnathostome morphology. *Entelognathus* combines osteichthyan-like marginal jaw bones with a conservative placoderm-like condition of the braincase, dermal skull roof and trunk armour, whereas the palatoquadrate shows similarities with that of crown gnathostomes. In other placoderms, the metapterygoid portion is low, and there is at most a very narrow commissural lamina<sup>33</sup>, whereas crown gnathostomes have a tall metapterygoid (making the palatoquadrate ‘cleaver-shaped’) and a developed commissural lamina confining the adductor muscle mesially<sup>12</sup> (Fig. 6b). In *Entelognathus*, a developed commissural lamina is present, but the metapterygoid portion is low. The low metapterygoid is linked to the possession of a broad arthrodire-like braincase with low side walls<sup>3,23</sup>, contrasting with the narrower and deeper braincase of crown gnathostomes. Such a character complement suggests that changes to the muscular organization and biting surfaces preceded the emergence of a cleaver-shaped palatoquadrate at or just before the crown gnathostome node.

### METHODS SUMMARY

To determine the phylogenetic position of *Entelognathus*, and to evaluate the existing gnathostome phylogenies, we conducted phylogenetic analyses (parsimony approach and Bayesian inference) using a modified data set with 253 characters and 75 taxa. Parsimony-based results place *Entelognathus* in a polychotomy with

arthrodires, ptyctodonts and crown gnathostomes. Unexposed or partially exposed structures of the holotype and a cheek-palatoquadrate complex were examined using X-ray micro-computerized tomography. The specimens in Figs 2, 4a, e and 5 were coated with ammonium chloride sublimate.

**Online Content** Any additional Methods, Extended Data display items and Source Data are available in the online version of the paper; references unique to these sections appear only in the online paper.

**Received 6 January; accepted 29 August 2013.**

**Published online 25 September 2013.**

- Moy-Thomas, J. A. & Miles, R. S. *Palaeozoic Fishes* (Chapman & Hall, 1971).
- Jarvik, E. *Basic Structure and Evolution of Vertebrates* Vol. 1 (Academic, 1980).
- Goujet, D. F. Placoderm interrelationships: a new interpretation, with a short review of placoderm classifications. *Proc. Linn. Soc. N. S. W.* **107**, 211–243 (1984).
- Gardiner, B. G. The relationship of placoderms. *J. Vertebr. Paleontol.* **4**, 379–395 (1984).
- Maisey, J. G. Heads and tails: a chordate phylogeny. *Cladistics* **2**, 201–256 (1986).
- Schultze, H.-P. in *The Skull* Vol. 2 (eds Janke, J. & Hall, B. K.) 189–254 (Univ. Chicago Press, 1993).
- Janvier, P. *Early Vertebrates* (Oxford Univ. Press, 1996).
- Young, G. C. Placoderms (armored fish): dominant vertebrates of the Devonian period. *Annu. Rev. Earth Planet. Sci.* **38**, 523–550 (2010).
- Long, J. A. *The Rise of Fishes: 500 Million Years of Evolution* 2nd edn (John Hopkins Univ. Press, 2011).
- Gross, W. Peut-on homologuer les os des Arthrodires et des Téléostomes? *Colloq. Int. CNRS* **104**, 69–74 (1962).
- Young, G. C. The relationships of placoderm fishes. *Zool. J. Linn. Soc.* **88**, 1–57 (1986).
- Schaeffer, B. in *Problèmes actuels de Paléontologie-Evolution des Vertébrés* Vol. 218 (ed. Lehman, J. P.) 101–109 (Actes du Colloque International CNRS, 1975).
- Goujet, D. F. in *Major Events in Early Vertebrate Evolution: Palaeontology, Phylogeny, Genetics and Development* (ed. Ahlberg, P. E.) 209–222 (Taylor & Francis, 2001).
- Johanson, Z. Vascularization of the osteostracan and antiarch (Placodermi) pectoral fin: similarities, and implications for placoderm relationships. *Lethaia* **35**, 169–186 (2002).
- Brazeau, M. D. The braincase and jaws of a Devonian 'acanthodian' and modern gnathostome origins. *Nature* **457**, 305–308 (2009).
- Davis, S. P., Finarelli, J. A. & Coates, M. I. *Acanthodes* and shark-like conditions in the last common ancestor of modern gnathostomes. *Nature* **486**, 247–250 (2012).
- Zhu, M. *et al.* Fossil fishes from China provide first evidence of dermal pelvic girdles in osteichthyans. *PLoS ONE* **7**, e35103 (2012).
- Zhu, M., Yu, X.-B. & Janvier, P. A primitive fossil fish sheds light on the origin of bony fishes. *Nature* **397**, 607–610 (1999).
- Zhu, M. & Schultze, H.-P. in *Major Events in Early Vertebrate Evolution: Palaeontology, Phylogeny, Genetics and Development* (ed. Ahlberg, P.) 289–314 (Taylor & Francis, 2001).
- Zhu, M. *et al.* The oldest articulated osteichthyan reveals mosaic gnathostome characters. *Nature* **458**, 469–474 (2009).
- Gardiner, B. G. The relationships of the palaeoniscid fishes, a review based on new specimens of *Mimia* and *Moythomasia* from the Upper Devonian of western Australia. *Bull. Br. Mus. Nat. Hist. Geol.* **7**, 173–428 (1984).
- Forey, P. L. & Gardiner, B. G. Observations on *Ctenurella* (Ptyctodontida) and the classification of placoderm fishes. *Zool. J. Linn. Soc.* **86**, 43–74 (1986).
- Stensiö, E. A. Anatomical studies on the arthrodiran head. Part 1. Preface, geological and geographical distribution, the organization of the head in the Dolichotheoraci, Coccosteomorphi and Pachyosteomorphi. Taxonomic appendix. *Kungl. Svenska Vetenskap. Hand.* **9**, 1–419 (1963).
- Zhao, W.-J. & Zhu, M. Siluro-Devonian vertebrate biostratigraphy and biogeography of China. *Palaeoworld* **19**, 4–26 (2010).
- Zhu, M., Liu, Y.-H., Jia, L.-T. & Gai, Z.-K. A new genus of eugaleaspidiforms (Agnatha: Galeaspidia) from the Ludlow, Silurian of Qujing, Yunnan, southwestern China. *Vertebr. Palasiat.* **50**, 1–7 (2012).
- Denison, R. H. in *Handbook of Paleichthyology* Vol. 2 (ed. Schultze, H.-P.) 1–128 (Gustav Fischer, 1978).
- Goujet, D. F. *Sigaspidis*, un nouvel arthrodire du Dévonien inférieur du Spitsberg. *Palaeontogr. A* **143**, 73–88 (1973).
- Liu, Y.-H. in *Early Vertebrates and Related Problems of Evolutionary Biology* (eds Chang, M.-M., Liu, Y.-H. & Zhang, G.-R.) 139–177 (Science Press, 1991).
- Burrow, C. J., Newman, M. J., Davidson, R. G. & den Blaauwen, J. L. Sclerotic plates or circumorbital bones in early jawed fishes? *Palaeontology* **54**, 207–214 (2011).
- Goujet, D. F. *Les Poissons Placodermes du Spitsberg. Arthrodires Dolichotheoraci de la Formation de Wood Bay (Dévonien Inférieur)* (CNRS, 1984).
- Trinajstić, K., Long, J. A., Johanson, Z., Young, G. & Senden, T. New morphological information on the ptyctodontid fishes (Placodermi, Ptyctodontida) from western Australia. *J. Vertebr. Paleontol.* **32**, 757–780 (2012).
- Friedman, M. & Brazeau, M. D. A reappraisal of the origin and basal radiation of the Osteichthyes. *J. Vertebr. Paleontol.* **30**, 36–56 (2010).
- Young, G. C. New information on the structure and relationships of *Buchanosteus* (Placodermi: Euarthrodira) from the Early Devonian of New South Wales. *Zool. J. Linn. Soc.* **66**, 309–352 (1979).
- Schultze, H.-P. & Cumbaa, S. L. in *Major Events in Early Vertebrate Evolution: Palaeontology, Phylogeny, Genetics and Development* (ed. Ahlberg, P. E.) 315–332 (Taylor & Francis, 2001).
- Botella, H., Blom, H., Dorka, M., Ahlberg, P. E. & Janvier, P. Jaws and teeth of the earliest bony fishes. *Nature* **448**, 583–586 (2007).

**Supplementary Information** is available in the online version of the paper.

**Acknowledgements** We thank M.-M. Chang, J. Long, G. Young, D. Goujet and J.-Q. Wang for discussions, X.-F. Lu, J. Zhang and C.-H. Xiong for specimen preparation, Y.-M. Hou for X-ray micro-computerized tomography. This work was supported by the Major State Basic Research Projects (2012CB821902) of MST of China, and the National Natural Science Foundation of China (40930208). P.E.A. and Q.Q. were supported by ERC Advanced Investigator Grant 233111 and a Wallenberg Scholarship from the Knut and Alice Wallenberg Foundation, both awarded to P.E.A.

**Author Contributions** M.Z. conceived the project. M.Z., W.Z., L.J., Y.Z., J.L. and T.Q. did the fieldwork. M.Z., P.E.A., T.Q., J.L., Q.Q., B.C., X.Y. and H.B. conducted the phylogenetic analyses. J.L., P.E.A. and M.Z. performed computerized tomography restorations. M.Z., P.E.A., X.Y. and B.C. discussed the results and prepared the manuscript.

**Author Information** The LSIDs urn:lsid:zoobank.org:pub:1CE67C34-52CC-4CEF-B731-DF1A4E85DE4B (article), urn:lsid:zoobank.org:act:D88DD67F-1159-4E7E-AE4C-814249337351 (genus), and urn:lsid:zoobank.org:act:77F76728-FBC1-407D-B2C1-1C5D5BF9B59C (species) have been deposited in ZooBank. Reprints and permissions information is available at [www.nature.com/reprints](http://www.nature.com/reprints). The authors declare no competing financial interests. Readers are welcome to comment on the online version of the paper. Correspondence and requests for materials should be addressed to M.Z. (zhumin@ivpp.ac.cn).

## METHODS

**Phylogenetic analysis.** To determine the position of *Entelognathus primordialialis* gen. et sp. nov., and to evaluate the impact of its characters on gnathostome phylogeny, we conducted phylogenetic analyses using a modified data set comprising a total of 253 characters and 75 taxa (see Supplementary Information for details). This data set (hereafter referred to as the full data set) is based on a previous one<sup>16</sup>, with revised codings for 29 of the original 138 characters, and with the addition of 115 characters and 15 taxa, including *Entelognathus*. We also analysed subsets of the full data set to detect the effect of including *Entelognathus* and the effect of revising codings, adding characters and adding taxa.

To test the overall homology hypothesis between placoderm and osteichthyan dermal skeletons properly, we followed the precedent of refs 15 and 16 in mostly using neutral descriptive codings for dermal bone characters that potentially span the placoderm–osteichthyan divide. For example, our character 161 is defined as ‘number of marginal bones alongside paired median skull roofing bones over the otico-occipital division of braincase’, without specifically addressing the relationship between the osteichthyan (tabular, supratemporal) and placoderm (anterior paranuchal, marginal) nomenclatures for bones in this position. This conservative coding strategy is appropriate for the initial phylogenetic assessment of a putative transitional form like *Entelognathus*.

The character data entry and formatting were performed in Mesquite 2.5 (ref. 36). All characters were treated as unordered, and weighted equally. The data set was subjected to parsimony analysis in PAUP\* 4.0b10 (ref. 37). Two agnathan taxa (Galeaspida and Osteostraci) were used as the outgroup. Tree searches were conducted using the heuristic algorithm, with 1,000 (full data set and subset 3) or 10,000 (subsets 1–2) random addition sequence replicates, and with ‘maxtrees’ set to ‘automatically increase’. Bremer decay indices were obtained using command files composed by TreeRot<sup>38</sup> in conjunction with the heuristic search algorithm in PAUP\*. Bootstrap values were calculated from 1,000 pseudoreplicates using the heuristic search option in PAUP\* (random addition sequence with 10 replicates).

For the full data set, Bayesian inference analysis was conducted with MrBayes 3.1.2 (refs 39, 40). Galeaspida was set as the outgroup, and the codings showing polymorphism were changed to ‘?’. Priors were kept at their default settings for standard (= morphological) analyses. The analysis was run for 10<sup>7</sup> generations to ensure that the average standard deviation of split frequencies is below 0.01 (an indication for convergence of two runs or stationarity). Samples were taken every 10<sup>2</sup> generations, resulting in a total of 10<sup>5</sup> samples for each of the parallel analyses. The first 2.5 × 10<sup>4</sup> samples for each run, representing the ‘burn-in’ period, were discarded. The 50% majority-rule consensus tree was computed for the sampled generations.

**X-ray micro-computerized tomography.** The scanning was carried out using the 225 kV micro-computerized tomography (developed by the Institute of High Energy Physics, Chinese Academy of Sciences (CAS)) at the Key Laboratory of Vertebrate Evolution and Human Origins, CAS. The specimen was scanned with beam energy of 130 kV and a flux of 90 μA at a detector resolution of 10.8 μm per pixel using a 720° rotation with a step size of 0.5° and an unfiltered aluminium reflection target. A total of 1,440 transmission images were reconstructed in a 2,048 × 2,048 matrix of 1,563 slices using a two-dimensional reconstruction software developed by the Institute of High Energy Physics, CAS. The three-dimensional reconstructions were created in Mimics (version 14.12), and images of the reconstructions were exported from Mimics and finalized in Adobe Photoshop and Adobe Illustrator.

36. Maddison, W. P. & Maddison, D. R. *Mesquite: A Modular System For Evolutionary Analysis* v. 2.5 (<http://mesquiteproject.org>, 2008).
37. Swofford, D. L. *PAUP\*: Phylogenetic analysis using parsimony (\* and other methods)*, version 4.0b 10 (Sinauer Associates, 2003).
38. Sorenson, M. D. *TreeRot. Program and documentation* v. 2 (Boston Univ., 1999).
39. Ronquist, F. & Huelsenbeck, J. P. MrBayes 3: Bayesian phylogenetic inference under mixed models. *Bioinformatics* **19**, 1572–1574 (2003).
40. Huelsenbeck, J. P. & Ronquist, F. MrBayes: Bayesian inference of phylogenetic trees. *Bioinformatics* **17**, 754–755 (2001).